



Novel Cu(II)-quinoline carboxamide complexes: Structural characterization, cytotoxicity and reactivity towards 5'-GMP

Junyong Zhang¹, Xiaokang Ke¹, Chao Tu¹, Jun Lin¹, Jian Ding², Liping Lin², Hoong-Kun Fun³, Xiaozeng You¹ & Zijian Guo^{1,*}

¹State Key Laboratory of Coordination Chemistry, Coordination Chemistry Institute, Nanjing University, 210093 Nanjing, P.R. China; ²Division of Anti-tumor Pharmacology, State Key Laboratory for New Drug Research, Shanghai Institute of Materia Medica, Shanghai Institutes for Biological Sciences, Chinese Academy of Sciences, Shanghai 200031, P.R. China; ³X-ray Crystallography Unit, School of Physics, Universiti Sains Malaysia, 11800 Penang, Malaysia; *Author for correspondence (E-mail: zguo@netra.nju.edu.cn)

Received 20 September 2002; accepted 27 September 2002; Published online February 2003

Key words: Cu(II) complexes, cytotoxicity, X-ray crystal structure, 5'-GMP

Abstract

Three new ligands, N-(8-quinolyl)pyridine-2-carboxamide (HL₁), N-(8-quinolyl)glycine-N'-Boc-carboxamide (HL₂), N-(8-quinolyl)-L-alanine-N'-Boc-carboxamide (HL₃), and their Cu(II) complexes have been synthesized. Crystallographic data reveal that complex I, [Cu(L₁)(Ac)(H₂O)], is penta-coordinated with a square-pyramidal geometry while complexes V [Cu(L₂')(H₂O)] and VI [Cu(L₃')(H₂O)] are tetra-coordinated to give square planar geometry. *In vitro* tests showed that the Cu(II) complexes with L₁ (I-IV) exhibited cytotoxicity at a concentration of 10⁻⁸ M against murine leukemia P-388 and human leukemia HL-60 cell lines, which is more potent than cisplatin. However, ligands HL₂ and HL₃ and their corresponding copper complexes demonstrated very weak *in vitro* activities towards the cell lines examined. ESMS data shows that complex I binds rapidly with 5'-GMP to form 1:1 and 2:2 adduct.

Introduction

The medicinal application of metal complexes has been a subject of great interest recently (*Chem Rev* 1999; Guo & Sadler 1999; Guo & Sadler 2000). Apart from the huge success of platinum-based drugs, some other metal compounds such as titanium and ruthenium complexes have shown some potential for chemotherapy. The toxicity of metallodrugs is problematic, therefore it is proposed that drugs based on essential metals may be less toxic, which has led to the investigation of copper-based drugs. Copper complexes have indeed demonstrated a wide range of pharmacological activity such as antiviral (Kaska *et al.* 1978; Ranford *et al.* 1993; West & Owens 1998), anticancer (Berners-Price *et al.* 1987; Moubaraki *et al.* 1999; Kong *et al.* 2000) and anti-inflammatory activity (Andrade *et al.* 2000). It was found that copper complexes often demonstrate enhanced biological activity

than the parent ligand alone (Mohindru *et al.* 1983; Ainscough *et al.* 1998).

One of the major intracellular targets of anticancer metallodrugs is DNA, therefore metal complexes that can bind to specific nucleobases of DNA are of interests in the development of antitumour agents. Copper complexes of 1, 10-phenanthroline and its derivatives are able to target DNA and have been used as DNA nuclease and as footprinting agents (Sigman, 1990; Mazumder *et al.* 1993; Sigman *et al.* 1993; Mahadevan & Palaniandavar 1998). Modification of 1,10-phenanthroline copper complex has resulted discovery of a series of anticancer agents casiopeinas (Ruiz-Ramirez *et al.* 1993, 1995; Vizcaya-Ruiz *et al.* 2000), and one of the complexes has been shown to induce apoptosis of murine leukemia cell lines (Vizcaya-Ruiz *et al.* 2000). Recently it was reported that some copper complexes with nitrogen containing heterocyclic ligand exhibited potent antitumor activity (Broomhead

et al. 1998; Madarász *et al.* 2000; Gokhale *et al.* 2001).

In this work we have designed three novel ligands, N-(8-quinolyl)-2-pyridinecarboxamide (Zhang *et al.* 2001) (HL₁), N-(8-quinolyl)glycine-N'-Boc-carboxamide (HL₂) and N-(8-quinolyl)-L-alanine-N'-Boc-carboxamide (HL₃) (Chart 1). In these ligands, the amino-quinoline moiety is condensed with either picolinic acid or amino acids glycine or L-alanine. We have investigated their chelating behavior towards Cu (II) in order to reveal the ligand influence on the geometry and subsequently the biological activity of the resulting complexes. The *in vitro* cytotoxicity of both ligands and their complexes against human leukaemia (HL-60), murine leukaemia (P388), human hepatoma (BEL-7402) and human lung adenocarcinoma (A-549) cell lines are reported.

Experimental section

Chemical materials

Cu(Ac)₂·H₂O, Cu(NO₃)₂·3H₂O and CuCl₂·2H₂O were received from the First Reagent Factory of Shanghai, Cu(ClO₄)₂·6H₂O was synthesized using CuCO₃ and HClO₄. Pyridine-2-carboxylic acid was purchased from Merck Corporation, di-tert-butyl dicarbonate and 8-aminoquinoline from Acros Organics. Guanosine-5'-monophosphate(5'-GMP), glycine, L-alanine and Calf thymus DNA were all from Sigma. All the solvents were of analytical reagent grade and used without further purification.

Spectroscopy

The infrared spectra were recorded on a Bruker VECTOR22 spectrometer as KBr pellets (4000–500 cm⁻¹), and elemental analysis was performed on a Perkin-Elmer 240C analytical instrument. Electron paramagnetic resonance spectra were recorded on an ER 200-D-SRC 10/12 spectrometer at X-band at 110 K. Electrospray mass spectra were recorded using an LCQ electron spray mass spectrometer (ESMS, Finnigan) by loading 1.0 μl of solution into the injection valve of the LCQ unit and then injecting into the mobile phase solution (50% of aqueous methanol) which was carried through the electrospray interface into the mass analyzer at a rate of 200 μl min⁻¹. The voltage employed at the electrospray needles was 5 kV, and the capillary was heated to 200 °C. A maximum ion injection time of 200 ms along with 10 scans

was set. Negative ion mass spectra were obtained. The predicted isotope distribution patterns for each of the complexes were calculated using the Isopro 3.0 program (Yergey 1983).

Preparations

The elemental analyses and yields of the compounds reported below are listed in Table 1.

N-(8-Quinolyl)pyridine-2-carboxamide (HL₁)

The ligand HL₁ was synthesized according to a literature method used for the preparation of carboxamides (Leung *et al.* 1991). To the mixture of 7 mmol pyridine-2-carboxylic acid (0.875 g) and one mol. equiv. of 8-aminoquinoline (1.009 g) in 70 ml pyridine was slowly added one mol. equiv. of triphenyl phosphite under stirring when the mixture was heated to 100 °C. The reaction was left stirring for 4 h and then cooled down to room temperature. The solvent was removed by rotary evaporator to give a pale brown solution. Colorless crystals were received from pyridine and ethanol. IR (KBr, cm⁻¹): ν_{CO}: 1687 (s). The crystal structure of HL₁ has been reported separately (Zhang *et al.* 2001).

N-(8-quinolyl)glycine-N'-Boc-carboxamide (HL₂) and N-(8-quinolyl)-L-alanine-N'-Boc-carboxamide (HL₃)

Ligand HL₂ was obtained by the following procedure. To a cooled solution of glycine (1.5 g, 20 mmol) in dioxane (16 ml), water (8 ml), 1 M NaOH (42 ml) and di-tert-butyl dicarbonate (4.8 g; 22 mmol) were added with stirring. The reaction was continued at 0 °C for 1 h, and then at room temperature for overnight. The resulting mixture was titrated with a saturated citric acid solution to adjust the pH to about 5, and then extracted with ethyl acetate (2 × 70 ml). The ethyl acetate layer was dried with Na₂SO₄ and concentrated to give pale yellow syrup of N-(tert-Butoxycarbonyl)glycine. Yield: 3.33 g, 95%. This product (1.23 g; 7 mmol) was dissolved in THF (35 ml), cooled to about -15 °C to which triethylamine (7 mmol) and ClCO₂Et (7 mmol) were added slowly by syringe. After stirring at -15 °C for 1 h, a cold (-15 °C) solution of 1 mol. equiv. of 8-aminoquinoline (1.008 g) in THF (15 ml) was added. The reaction was continued at -15 °C for 1 h and then at room temperature for overnight. The resulting mixture was filtered, and the filtrate was concentrated to give HL₂. IR (KBr, cm⁻¹): ν_{CO}: 1713 (s) and 1677 (s).

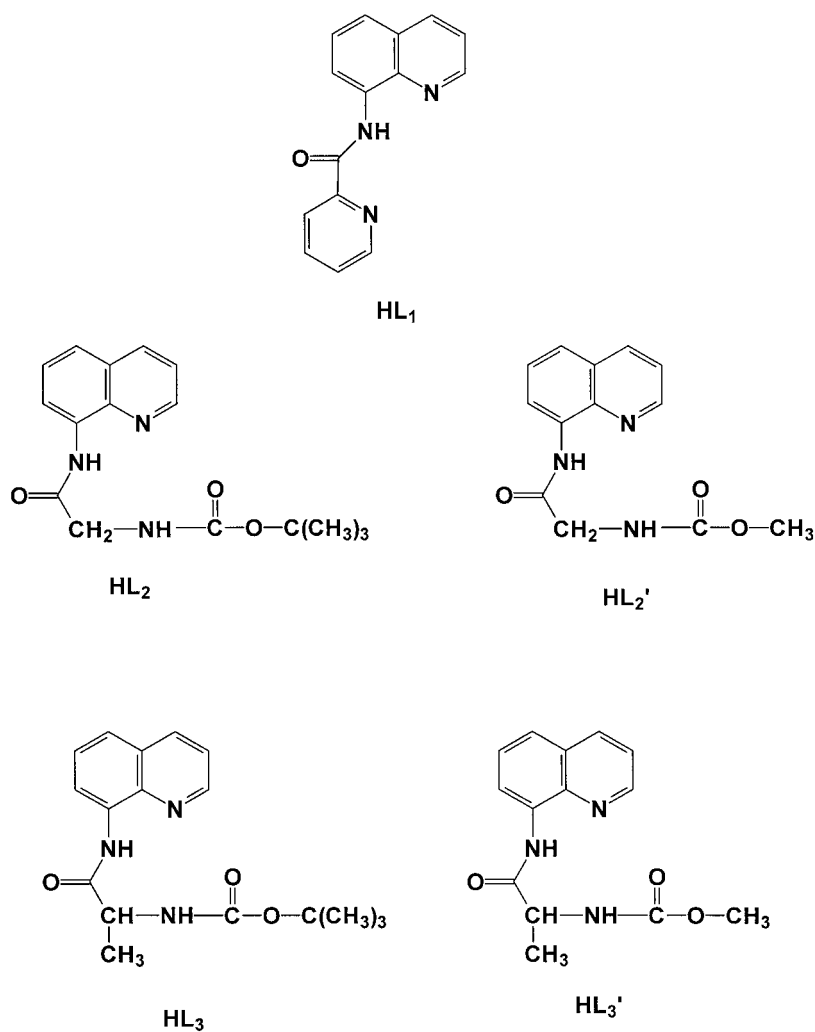


Chart. 1. Chemical structure of the novel ligands used for the preparation of the Cu(II) complexes.

Table 1. Elemental analysis of the compounds.

Compounds	Found (Calc.) (%)			Yield (%)
	C	H	N	
HL ₁	71.9(72.3)	4.43(4.42)	16.5(16.7)	71
HL ₂	63.5(63.8)	6.29(6.31)	14.7(14.0)	92
HL ₃	64.6(64.8)	6.68(6.67)	6.4(6.3)	90
Complex I	52.4(52.5)	3.85(3.86)	10.9(10.8)	72
Complex II	41.8(42.0)	2.79(2.80)	9.8(9.8)	75
Complex III	46.3(46.0)	3.04(3.07)	14.5(14.3)	80
Complex IV	49.0(49.3)	3.33(3.29)	11.4(11.5)	85
Complex V	46.3(46.1)	3.81(3.84)	12.2(12.4)	81
Complex VI	47.3(47.9)	3.74(3.71)	11.9(12.0)	78

Table 2. Crystal data and structure refinement for Complexes I, V and VI.

Complex	Complex I	Complex V	Complex VI
Empirical formula	C ₁₇ H ₁₅ CuN ₃ O ₄	C ₁₃ H ₁₃ N ₃ O ₄ Cu	C ₁₄ H ₁₆ N ₃ O ₄ Cu
Formula weight	388.86	338.80	352.83
Temperature/K	293(2)	293(2)	293(2)
Crystal size/mm	0.38 × 0.24 × 0.14	0.25 × 0.20 × 0.15	0.25 × 0.20 × 0.15
Crystal habit/color	Prism/Dark green	Prism/mauve	Prism/mauve
Crystal system	Monoclinic	Monoclinic	Monoclinic
Space group	P2 ₁ /n	P2 ₁ /n	P2 ₁
a/Å	8.364(1)	9.571(2)	7.852(2)
b/Å	14.025(1)	9.404(2)	7.778(2)
c/Å	14.144(1)	14.935(3)	23.164(5)
α/°	90	90	90
β/°	99.438(1)	107.489(4)	92.44(3)
γ/°	90	90	90
V/Å ³	1636.7(3)	1282.1(5)	1413.5(5)
Z	4	4	4
Calculated density/Mg m ⁻³	1.578	1.755	1.658
Absorption coefficient (mm ⁻¹)	1.362	1.724	1.568
F(000)	796	692	724
θ Range for data collection/°	2.06 to 28.27	2.26 to 28.18	2.60 to 28.27
Limiting indices	-11 ≤ h ≤ 10, -18 ≤ k ≤ 17, -12 ≤ l ≤ 18	-12 ≤ h ≤ 12, -12 ≤ k ≤ 12, -16 ≤ l ≤ 19	-10 ≤ h ≤ 9, -6 ≤ k ≤ 10, -30 ≤ l ≤ 14
Reflections collected	11461	7636	5301
Independent reflections	3999(R _{int} =0.0685)	2915(R _{int} =0.0730)	3909(R _{int} =0.0490)
Absorption correction	Empirical	Empirical	Empirical
Max. and min. Transmission	0.8322 and 0.6256	1 and 0.736	1 and 0.765
Data/restraints/parameters	3999/0/228	2915 / 0 / 191	3909 / 1 / 401
Goodness-of-fit on F ²	1.039	1.015	1.048
Final R indices [I > 2σ(I)]	R1=0.0421, WR2=0.0978	R1=0.0472, WR2=0.0793	R1=0.0438, WR2=0.0640
Largest diff. peak and hole/eÅ ⁻³	0.575 and -0.965	0.842 and -0.416	0.505 and -0.547
Refinement method	Full-matrix least-squares on F ²	Full matrix least-squares on F ²	Full-matrix least-squares on F ²

HL₃ was synthesized following the same procedure using the amino acid L-alanine as the starting material. IR (KBr, cm⁻¹): ν_{CO}: 1700 (s) and 1677 (s).

Complexes I - IV: [Cu(L₁)(X)(H₂O)] (X = Ac, ClO₄, NO₃ and Cl, respectively)

Complex I was prepared as follows. To a solution of Cu(Ac)₂·H₂O (0.2 mmol, 40 mg) in 2 ml methanol was added dropwise the solution of HL₁ (0.2 mmol, 49.8 mg) in 2 ml CH₃OH with stirring. The mixture was then refluxed for 2 h. Single crystals suitable for X-ray diffraction were obtained by slow evaporation of a methanol solution. IR (KBr, cm⁻¹):

ν_{OH}: ~3388 (m, b), ν_{CO}: 1621 (s). λ_{max}, nm (ε) (MeOH): 252 (33.26 × 10³ M⁻¹ cm⁻¹), 359 (9.473 × 10³ M⁻¹ cm⁻¹), 614.5 (37.68 M⁻¹ cm⁻¹).

Complex II, III and IV were also synthesized according to the same procedure using Cu(ClO₄)₂·6H₂O (74.1 mg, 0.2 mmol), Cu(NO₃)₂·3H₂O (48.4 mg, 0.2 mmol) and CuCl₂·2H₂O (34.1 mg, 0.2 mmol), respectively, as the starting salt. IR (KBr, cm⁻¹): complex II: ν_{OH}: ~3474 (m, b), ν_{CO}: 1630 (s); complex III: ν_{OH}: ~3423 (m, b), ν_{CO}: 1630 (s); Complex IV: ν_{OH}: ~3447 (m, b), ν_{CO}: 1642 (s).

Complexes [Cu(L₂')(H₂O)] (V) and [Cu(L₃')(H₂O)] (VI)

These two complexes were synthesized following the same procedure as that for complex I using HL₂ or HL₃ as the starting ligand. It should be noted that during the refluxing process, the tertiary butyl ester was changed to methyl ester, i.e. L₂ to L₂' and L₃ to L₃' (Chart 1). Single crystals suitable for X-ray diffraction were obtained by slow evaporation of a methanol solution. IR for complex V (KBr, cm⁻¹): ν_{OH}: ~ 3425 (m, b), ν_{CO}: 1598 (s) and 1570 (s). IR for complex VI (KBr, cm⁻¹): ν_{OH}: ~ 3425 (m, b), ν_{CO}: 1593 (s) and 1550 (s).

X-Ray structure determination

The raw data of complexes I, V and VI were all collected on a Siemens SMART CCD diffractometer at room temperature. The collected data were reduced using the program SAINT (Sheldrick 1996) and empirical absorption correction was carried out using the SADABS (Sheldrick 1996) Program. The structure was solved by direct methods that revealed the position of all non-hydrogen atoms and refined using the full-matrix least-squares method on F²_{obs} by using the SHELXTL (Sheldrick 1996) software package. All non-H atoms were anisotropically refined. Hydrogen atoms on carbons were located geometrically, hydrogen atoms of water molecules were found from difference Fourier Map, all the hydrogen atoms were refined in riding mode. The molecular graphics were created using SHELXTL. Atomic scattering factors and anomalous dispersion correction were taken from the International Table for X-ray Crystallography (Wilson 1992).

Cytotoxicity assays

The cytotoxicities of HL₁, HL₂, HL₃ and copper (II) complexes (I–VI) were investigated as follows. Tumor cell lines were grown in RPMI-1640 medium supplemented with 10% (vol/vol) heat-inactivated fetal bovine serum, 2 mmol/l glutamine, 100 U/ml penicillin, and 100 μg/ml streptomycin (GIBCO, Grand Island, NY) in a highly humidified atmosphere of 95% air with 5% CO₂ at 37 °C.

Growth inhibitory effect of copper complexes on the murine leukemia P-388 and human leukemia HL-60 cells was measured by the microculture tetrazolium [3-(4,5-dimethylthiazol-2-yl)-2,5-diphenyl-tetrazolium bromide, MTT] assay (Alley *et al.* 1988). Briefly,

Cells in 100 μl culture medium were plated in each well of 96-well plates (Falcon, Calif.). The cells were treated in triplicate with grade concentrations of the three ligands, their copper complexes and the reference drug cisplatin at 37 °C for 48 h. A 20 μL aliquot of MTT solution (5 mg/ml) was added directly to all the appropriate wells. The culture was then incubated for 4 h. Then 100 μl 'triplex solution' (10% SDS-5% isobutanol-12 mM HCl) was added. After the plates were incubated at 37 °C overnight, they were measured by the absorbance at 570 nm using a multiwell spectrophotometer (VERSA Max, Molecular Devices, USA).

For human hepatocarcinoma BEL-7402, lung adenocarcinoma A-549 and colon adenocarcinoma HCT-116 cell lines, the growth inhibition was analyzed by the sulforhodamine B (SRB) assay (Skehan *et al.* 1990). Briefly, adherent cells in a 100 μl medium were seeded in 96-well plates and allowed to attach for 24 h before drug addition. The cell densities were selected based on preliminary tests to maintain control cells in an exponential phase of growth during the period of the experiment and to obtain a linear relationship between the optical density (OD) and the number of viable cells. Each cell line was exposed to grade concentrations of the compounds at desired final concentrations for 72 h and each concentration was tested in triplicate wells. After exposure, cells were fixed by gentle addition of 100 μl of cold (4 °C) 10% trichloroacetic acid to each well, followed by incubation at 4 °C for 1 h. Plates were washed with deionized water five times and allowed to air dry. Cells were stained by addition of 100 μl SRB solution (0.4% SRB (w/v) in 1% acetic acid (v/v) to wells for 15 min. Then plates were quickly washed five times with 1% acetic acid to remove any unbound dye and allowed to air dry. Bound dye was solubilized with 10 mmol ml⁻¹ Tris (pH 10.5) prior to reading plates. The OD (Optical Density) value was read on a plate reader (Molecular Devices, VERSAmax) at a wavelength of 515 nm. Media and DMSO control wells, in which compounds were absent, were included in all the experiments. The growth inhibitory rate of treated cells was calculated by (OD_{control} – OD_{test}) / OD_{control} × 100%.

The reaction of complex I with nucleotide 5'-GMP

To the solution of complex I (15.5 mg, 0.04 mmol) in 3 ml methanol one mol. equiv. of 5'-GMP (16.3 mg) in 3.5 ml H₂O was added with stirring. The reaction was continued for 1 h at room temperature. The pH

Table 3. Selected bond distances (Å) and angles (°) for Complex I.

Cu(1)-N(1)	2.026(2)	Cu(1)-N(2)	1.943(2)
Cu(1)-N(3)	2.018(2)	Cu(1)-O(2)	2.309(2)
Cu(1)-O(3)	1.958(2)	N(1)-C(5)	1.350(3)
C(5)-C(6)	1.504(4)	C(6)-N(2)	1.341(3)
N(2)-C(7)	1.387(3)	N(3)-C(15)	1.364(3)
N(3)-C(14)	1.325(3)	C(6)-O(1)	1.243(3)
O(2)-Cu(1)-N(1)	95.11(7)	N(1)-Cu(1)-N(2)	81.36(8)
O(2)-Cu(1)-N(2)	96.47(8)	N(2)-Cu(1)-N(3)	81.92(8)
O(2)-Cu(1)-N(3)	91.63(8)	N(3)-Cu(1)-O(3)	98.07(8)
O(2)-Cu(1)-O(3)	90.95(7)	O(3)-Cu(1)-N(2)	170.58(7)
O(3)-Cu(1)-N(1)	97.62(8)	N(3)-Cu(1)-N(1)	162.57(8)
N(1)-C(5)-C(6)	116.1(2)	C(5)-C(6)-N(2)	111.4(2)
C(6)-N(2)-C(7)	125.6(2)	C(5)-C(6)-O(1)	120.4(2)

value of the above solutions is 6.0 and no buffer was used. ESMS were recorded about 1 h after the mixing of complex I with 5'-GMP.

Results and discussion

Crystallography of complexes I, V and VI

The crystal data, data collection, structural solution and refinement parameters for complexes I, V and VI are summarized in Table 2.

The selected bond distances and angles of complex I are listed in Table 3. As can be seen from Figure 1, Cu(II) is bonded to the acetate ligand through O(3) and to the L through three nitrogen atoms [pyridine N(1), amide N(2) and quinoline N(3)] with N(1) and N(2) being in *cis* position. A water molecule is coordinated to Cu(II) through O(2), therefore, in complex I Cu(II) adopts a standard square-pyramidal arrangement with O(2) occupying its apex and with N(1), N(2), N(3) and O(3) lying on the basal plane. Ligand L₁ may be considered as the basic plane of the molecule and the mean deviation from CuN₃O plane [Cu(1)-N(1)-N(2)-N(3)-O(3)] is 0.04 Å, while the Cu(II) atom show deviations of the order of -0.05 Å away from the basic plane. The approximately square-planar coordination of the Cu(II) atom generates two five-membered rings and the torsion angles of Cu(1)-N(1)-C(5)-C(6), Cu(1)-N(2)-C(6)-C(5), Cu(1)-N(2)-C(7)-C(15) and Cu(1)-N(3)-C(15)-C(7) are -3.2(3)°, -1.6(3)°, -1.2(3)° and 0.3(3)°, respectively.

Table 4. Selected bond distances (Å) and angles (°) for Complex V and Complex VI.

Bonds and angles	Complex V	Complex VI	A
Cu(1)-N(1)	1.986(3)	1.997(5)	1.982(4)
Cu(1)-N(2)	1.906(3)	1.911(4)	1.917(4)
Cu(1)-N(3)	1.933(3)	1.927(5)	1.921(4)
Cu(1)-O(4)	1.950(2)	1.938(4)	1.951(4)
C(1)-N(2)	1.405(4)	1.380(7)	v1.391(6)
N(2)-C(10)	1.339(4)	1.318(7)	1.321(7)
C(10)-O(1)	1.241(4)	1.253(7)	1.237(7)
C(11)-N(3)	1.472(4)	1.448(6)	1.453(6)
N(3)-C(12)	1.310(4)	1.327(8)	1.310(8)
C(12)-O(2)	1.248(4)	1.209(9)	1.221(8)
N(1)-Cu(1)-N(2)	83.32(11)	82.90(18)	83.20(18)
N(1)-Cu(1)-O(4)	96.45(10)	98.18(18)	95.40(18)
N(2)-Cu(1)-N(3)	84.91(11)	83.55(18)	83.67(19)
N(2)-Cu(1)-O(4)	177.11(11)	178.12(17)	178.34(19)
N(3)-Cu(1)-O(4)	95.36(10)	95.31(18)	97.78(19)
C(10)-C(11)-N(3)	111.7(3)	109.1(5)	109.7(5)

The three Cu-N bond distances are in the normal ranges according to the corresponding bond and are comparable to those in [Cu(bpb)(H₂O)] (Chapman *et al.* 1980) and [Cu(APPy)] (Rowland *et al.* 2001). However, the average Cu-N (pyridine or quinoline) bond lengths [2.022(2) Å] are significantly longer (0.08 Å) than the Cu-N (amide) bond in the same compound, this may be due to the different electron-donating abilities of amide N and heterocyclic N atoms (Zhang *et al.* 2001). The Cu-O(3) (acetate) bond length is in the expected ranges. As can be noted, the coordination of Cu (II) did not change significantly the bond lengths of the ligand L₁. The water molecule forms hydrogen bonds with carbonyl oxygen atoms of adjacent chelate molecules. The D...A separations are 2.790(4) and 2.799(4) Å for O(2)·O(1A), O(2)·O(4B), respectively (symmetry code A: -0.5+x, 0.5-y, -0.5+z. B: 0.5-x, -0.5+y, 0.5-z). The D-H·A angles are ca. 172° and 175° for O(2)-H(2B)·O(1A), O(2)-H(2C)·O(4B), respectively. There are strong intermolecular $\pi - \pi$ stacking interactions between the quinolyl and quinolyl rings, quinolyl and pyridyl rings in neighboring molecules to stabilize the crystal packing. The intermolecular $\pi - \pi$ stacking interaction were characterized by the dihedral angles of 0° and 3.8° for pairs of stacked quinolyl rings, and pyridyl and quinolyl rings respectively, and the shortest intermolecular atom-atom separations of these stacking

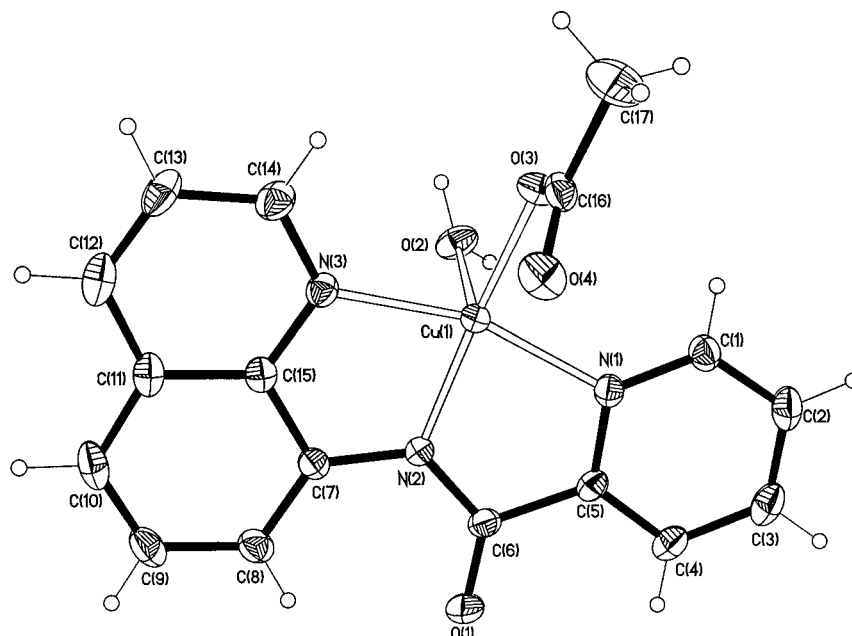


Fig. 1. The structure of complex I with atom numbering scheme. Thermal ellipsoids are drawn at 50% probability.

rings are 3.42 Å, 3.39 Å for C(7)–C(11C), C(12)–C(1D), respectively (symmetry codes, C: $-x, 1-y, 1-z$, D: $-1+x, y, z$).

The selected bond distances and angles of complex V and VI are listed in Table 4. Figures 2 and 3 show the ORTEP drawings of the asymmetric unit with an atom-numbering scheme of complex V and VI, respectively. Cu(II) in complex V as well as in complex VI is bonded to a water molecule through O(4) and to the ligand through three nitrogen atoms [quinoline N(1), amide N(2) and N(3)] with N(2) and N(3) being in *cis* position. Thus in the two complexes, Cu(II) both adopt standard planar arrangement with N(1), N(2), N(3) and O(4) lying on the basic plane. The mean deviations from CuN₃O plane [Cu(1)–N(1)–N(2)–N(3)–O(4)] are 0.0276 Å to complex V and 0.0242 Å to complex VI, while the Cu(II) ions show deviations of the order of -0.0138 Å for V and 0.0098 Å for VI away from the basic plane separately. While complexes I and V crystallized in the space group P2₁/n, chiral complex VI crystallized in chiral space group P2₁, with two independent molecules in the unit cell that adopt head-to-tail configuration.

As can be seen from Table 4, all the corresponding bonds and angles in the two complexes are similar to each other, and comparable to those in complex I. The Cu–O (aqua) in complex I is significantly longer than that in complexes V and

VI due to the Jahn-Teller effect. The water molecule forms both intra- and inter-molecular hydrogen bonds with carbonyl oxygen atoms. In complex V, the D⋯A separations are 2.580 and 2.634 Å for O(4)⋯O(2) and O(4)⋯O(1A), respectively (symmetry code, A: $0.5-x, -0.5+y, 0.5-z$), the D–H⋯A angles are ca. 163° and 172° for O(4)–H(4B)⋯O(2), O(4)–H(4C)⋯O(1A) respectively. In complex VI, the D⋯A separations are 2.566 Å, 2.638 Å, 2.542 Å and 2.671 Å for O(4)⋯O(2), O(4)⋯O(1B), O(4A)⋯O(2A) and O(4A)⋯O(1AB), respectively (symmetry code, B: $x, y-1, z$), the D–H⋯A angles are ca. 148°, 169°, 145° and 169° for O(4)–H(4C)⋯O(2), O(4)–H(4B)⋯O(1B), O(4A)–H(4AC)⋯O(2A) and O(4A)–H(4AB)⋯O(1AB), respectively.

It is interesting to note that Cu (II) in complex I is penta-coordinated while in complexes V and VI is tetra-coordinated. Due to the Jahn-Teller effects, Cu (II) does not bind to the fifth and sixth ligands strongly, even aqua (Cotton & Wilkinson 1988). It is likely that very strong intra-molecular H-bonding between O(2) and O(4) in complexes V and VI stabilized the aqua-ligand which precludes the binding of acetate ligand and hence the aqua ligand in apical position. As it will be shown below, complex I also demonstrated very different cytotoxicity, compared to complexes V and VI, towards the cell lines examined.

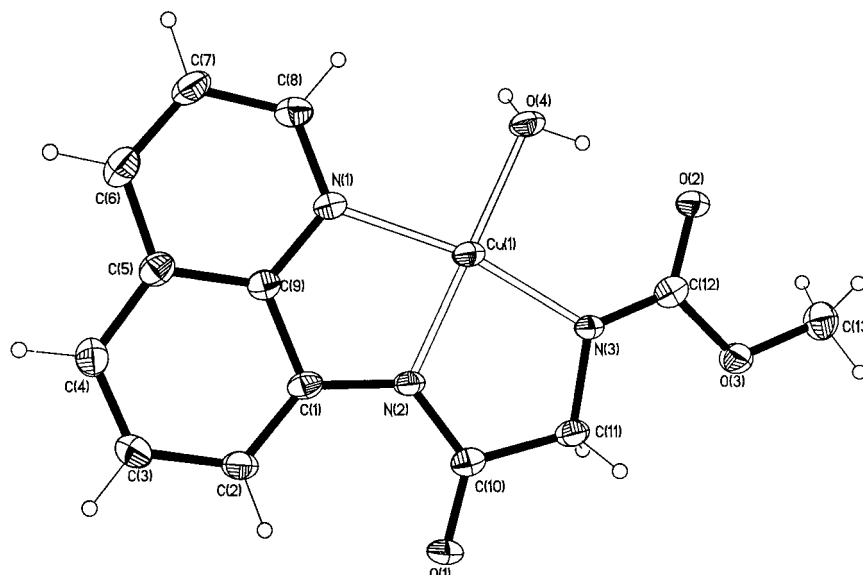


Fig. 2. The structure of complex V with atom numbering scheme. Thermal ellipsoids are drawn at 50% probability.

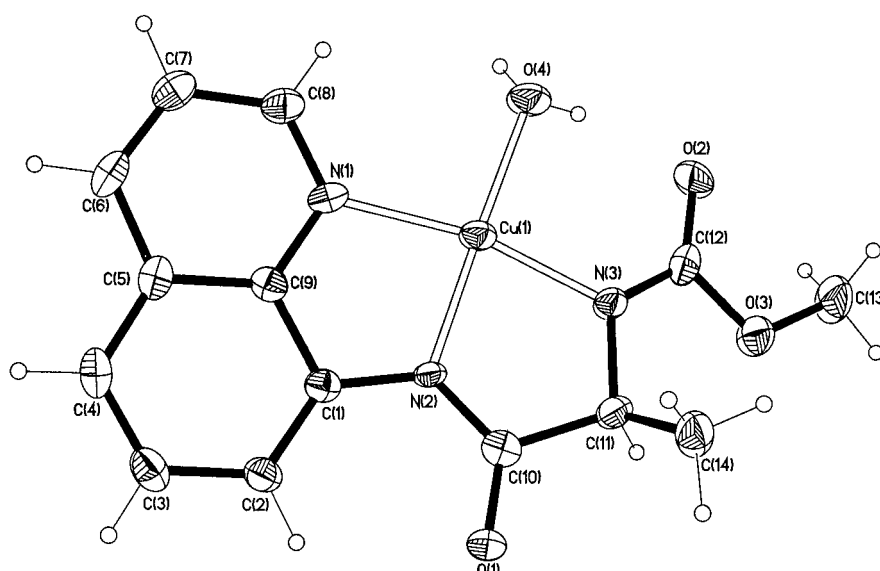


Fig. 3. The structure of complex V with atom numbering scheme. Thermal ellipsoids are drawn at 50% probability.

Biological activity

Figure 4 showed that both of HL₁ and complex I exhibited significant *in vitro* anticancer activities against the examined leukemia and human solid tumor cell lines. The two leukemia cell lines were more sensitive to HL₁ and complex I than the two solid tumor cell lines. At the concentration of 1×10^{-7} mol/l of HL₁ and complex I, the growth inhibition of both P-388 and HL-60 cells were above 50.0%, whereas those of A-549 and BEL-7402 cells were below 15.0%. Com-

plex I exhibited stronger *in vitro* antitumor activities than did the free ligand against three human tumor cell lines. In HL-60, A-549, and BEL-7402 cells, the growth inhibitory rates of complex I were 84.9, 12.6, and 15.0% whereas those of HL₁ were 74.2, 11.0, and 0.0%, respectively, at the same molarity concentration of 1×10^{-7} . It is notable that HL₁ and complex I exerted more potent cytotoxic activity than did cisplatin, a clinically-used metal-containing antitumor drug, in our test system (see Figure S1). Additionally,

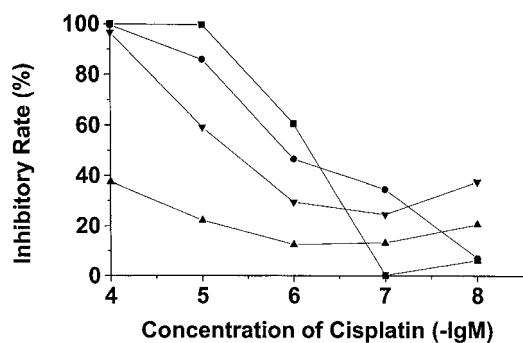


Fig. S1. Cytotoxic activity of cisplatin against tumor cell lines: [■]: Human leukaemia cells (HL-60), ●: Murine leukaemia cells (P388), ▲: Human liver cancer cells (BEL-7402), ▼: Human lung cancer cells (A-549)].

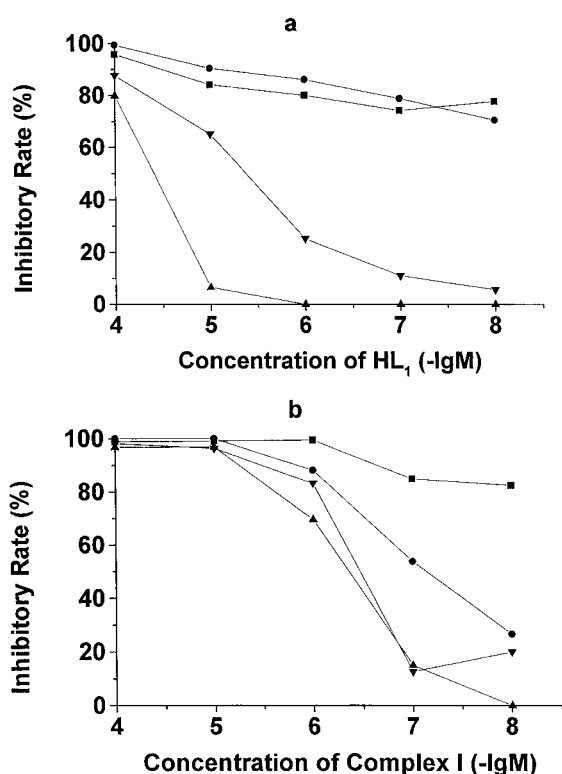


Fig. 4. Cytotoxic activity of HL₁ (a) and complex VI (b) against selected tumor cell lines: [■]: Human leukaemia cells (HL-60), ●: Murine leukaemia cells (P388), σ: Human liver cancer cells (BEL-7402), τ: Human lung cancer cells (A-549)].

their growth inhibition was in a dose-dependent manner as seen from Figure 4. As shown in Figure S2, complexes II, III and IV also exhibit potent *in vitro* cytotoxicity against the examined cell lines, suggesting that anions do not affect the activity of the Cu (II) complex. In contrast, ligands HL₂, HL₃ and their copper complexes (V and VI) are almost inactive to the

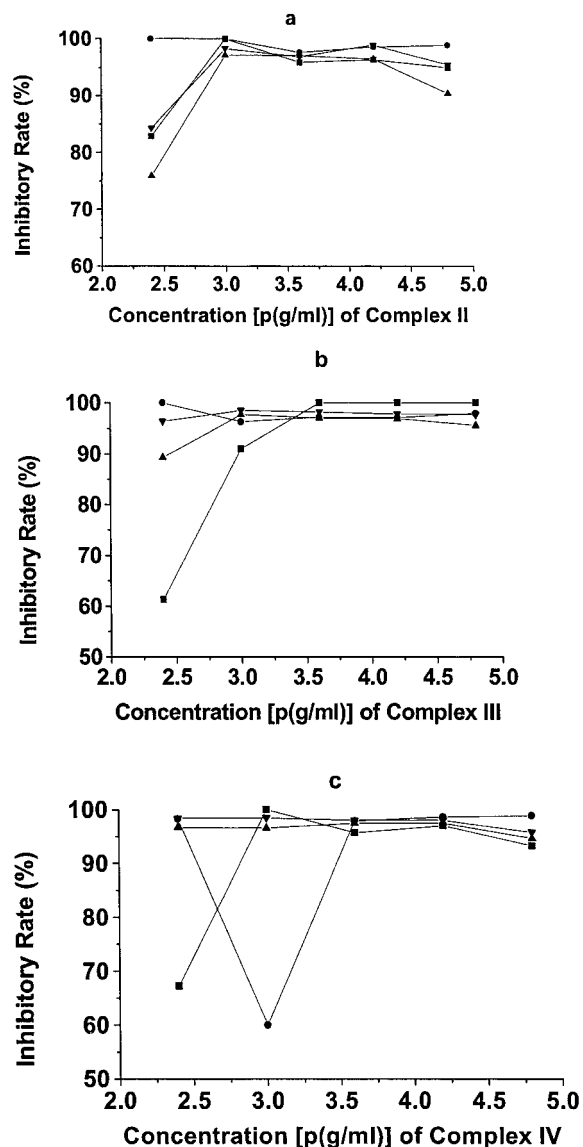


Fig. S2. Cytotoxic activity of complexes II (a), III (b) and IV (c) against selected tumor cell lines [p(g/ml) as $-\log$ (g/ml)]: [■]: Human leukaemia cells (HL-60), ●: Murine leukaemia cells (P388), ▲: Human liver cancer cells (BEL-7402), ▼: Humang lung cancer cells (A-549)].

examined cell lines, as shown in Figures S3 and S4. The activity differences between complex I and complexes V and VI may be correlated to the geometrical differences between them, as well as to the differences in functional groups.

Reactions of complex I with nucleotide 5'-GMP

As complex I shows very potent cytotoxicity against different tumor cell lines, its reactivity towards nu-

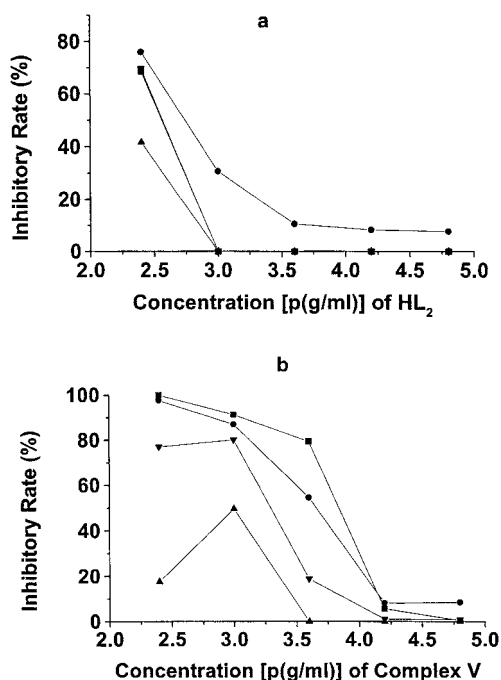


Fig. S3. Cytotoxic activity of HL₂ (a) and complex V (b) against selected tumor cell lines [p(g/ml) as $-\log$ (g/ml)]: [■]: Human leukaemia cells (HL-60), [●]: Murine leukaemia cells (P388), [▲]: Human liver cancer cells (BEL-7402), [▼]: Humang lung cancer cells (A-549)].

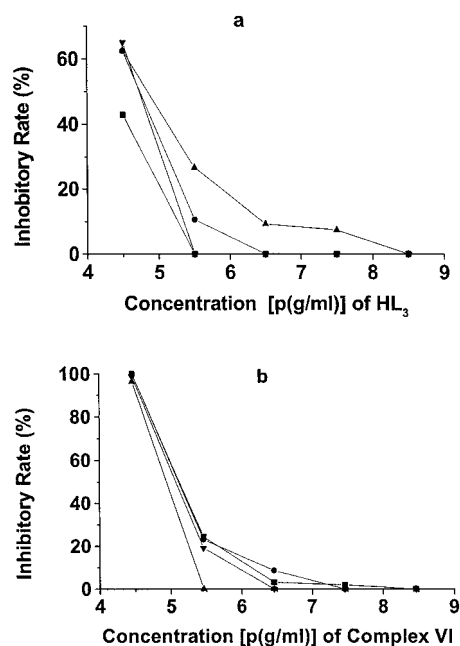


Fig. S4. Cytotoxic activity of HL₃ (a) and complex VI (b) against selected tumor cell lines [p(g/ml) as $-\log$ (g/ml)]: [■]: Human leukaemia cells (HL-60), [●]: Murine leukaemia cells (P388), [▲]: Human liver cancer cells (BEL-7402), [▼]: Humang lung cancer cells (A-549)].

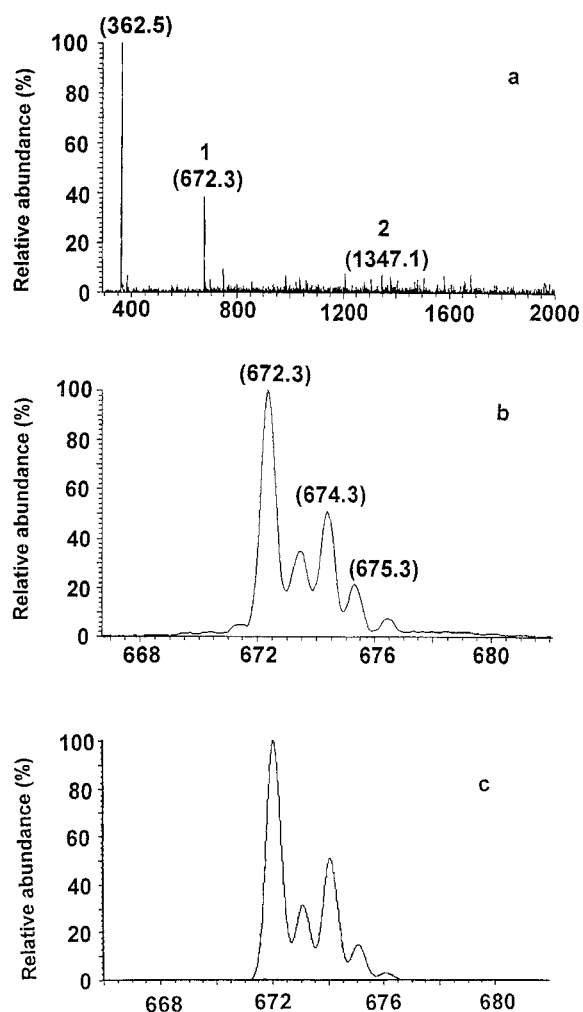


Fig. 5. (a) The ESMS spectrum of the solution of complex I and 5'-GMP 1 h after mixing; (b) The expanded spectrum of peak 1; (c) Calculated spectrum of peak 1.

cleotide 5'-GMP was investigated at aqueous solution. Upon mixing the solutions of complex I and 5'-GMP, pale green precipitates which designated as I-GMP were formed after a few hours after mixing. The IR spectrum of the precipitate was recorded, which shows the presence of phosphate bands at ~ 1080 and ~ 980 cm^{-1} , assignable to the stretching vibration of O-P-O and P-O-C, respectively (Cini & Pifferi 1999). The EPR data of complex I and I-GMP recorded at 110 K demonstrated that the coordination of complex I to 5'-GMP did not cause significant variation of the g values (I: g_1 , 2.05, g_2 , 2.10, g_3 , 2.13; I-GMP: g_1 , 2.03, g_2 , 2.08, g_3 , 2.18), suggesting the geometry around Cu (II) was kept unchanged.

The above reaction was also studied by ESMS spectrum. Figure 5a shows the ESMS spectrum of reaction mixture of complex I and 5'-GMP after 1 h reaction. As noted, all the isotopic peaks were separated by 1 unit and can be attributed to complexes with one negative charge. The highest peak that has a m/z value of 362.5 can be assigned to one negatively charged 5'-GMP (GMP^-). The major product of the reaction was peak 1 that has a m/z value of 672.3 and can be assigned to the complex $[\text{Cu}(\text{L}_1)(5'\text{-GMP})]^-$ (Figure 5b). The calculated molecular mass and the isotopic distribution match perfectly with the formula (Figure 5c). The m/z value and isotopic distribution of peak 2 (1347.1) corresponded to the formation of complex $[\text{Cu}_2(\text{L}_1)_2(5'\text{-GMP})_2]^-$, indicating that the association of $[\text{Cu}(\text{L}_1)(5'\text{-GMP})]^-$ occurred in solution. The self-stacking of nucleotides and their complexes has been well documented in the literature (for example, Bianchi *et al.* 2000).

All the data suggest that upon reacting with the nucleotide, complex I loses the aqua and acetate ligands which are possibly replaced by the nucleobase N and phosphate O donors. It is reported Cu (II) forms chelate complexes with N (7) of purine ring and with the phosphate group (Lüth *et al.* 1999). Recent calorimetric data confirm that 5'-GMP has the highest tendency to form the N (7) and phosphate macrochelation with Cu (II) compound compared to other nucleotides (Herrero & Terrón 2000).

In summary, we have shown the changing ligand from HL_1 to HL_2 and HL_3 , the resulting complexes with Cu (II) may adopt different coordination mode and geometry. Moreover, very different cytotoxicity was found for these complexes, among them complex I demonstrated the most potent activity. Complex I is more active than cisplatin in the tumor cell lines examined. We are currently investigating the binding mode of complex I towards DNA in order to elucidate the detailed mechanism of its antitumor activity.

Acknowledgements

We thank the financial supports from the National Natural Science Foundation of China for the Distinguished Young Scientists Fund (Grant No. 29925102), the Ministry of Education for SRFDP (No. 20010284029) and Mr Chenghui Xu and Ms Weiyi Yang for cytotoxicity assays. HKF would like to thank the Malaysian Government and Uni-

versiti Sains Malaysia for the research grant No: 305/PFIZIK/610961.

References

- Special issue on medicinal inorganic chemistry. 1999 *Chem Rev* **99**(9).
- Ainscough EW, Brodie AM, Denny WA, Finlay GJ, Ranford JD. 1998 Nitrogen, sulfur and oxygen donor adducts with copper(II) complexes of antitumor 2-formylpyridinethiosemicarbazone analogs: Physicochemical and cytotoxic studies. *J Inorg Biochem* **70**, 175–185.
- Alley MC, Scudiero DA, Monks A *et al.* 1988 Feasibility of drug screening with panels of human-tumor cell-lines using a microculture tetrazolium assay. *Cancer Res* **48**, 589–601.
- Andrade A, Namora SF, Woisky RG *et al.* 2000 Synthesis and characterization of a diruthenium-ibuprofenato complex: Comparing its anti-inflammatory activity with that of a copper(II)-ibuprofenato complex. *J Inorg Biochem* **81**, 23–27.
- Berners-Price SJ, Johnson RK, Mirabelli CK, Faucette LF, McCabe FL, Sadler PJ. 1987 Copper(I) complexes with bidentate tertiary phosphine ligands: Solution chemistry and antitumor activity. *Inorg Chem* **26**, 3383–3387.
- Bianchi EM, Sajadi SAA, Song B, Sigel H. 2000 Intramolecular stacking interactions in mixed ligand complexes formed by copper (II), 2,2'-bipyridine or 1,10-phenanthroline, and mono-protonated or deprotonated adenosine 5'-diphosphate (ADP^{3-}). Evaluation of isomeric equilibria. *Inorg Chim Acta* **300**, 487–498.
- Broomhead JA, Camm G, Sterns M, Webster L. 1998 Dinuclear complexes of first transition series metals with 4,4'-dipyrazolylmethane: characterization, DNA binding and anticancer properties. *Inorg Chim Acta* **271**, 151–159.
- Chapman RL, Stephens FS, Vagg RS. 1980 Studies on the Metal-Amide Bond. II*. The Crystal structure of the Deprotonated Copper (II) complex of N,N'-Bis-(2'-pyridinecarboxamide)-1,2-benzene. *Inorg Chim Acta* **43**, 29–33.
- Cini R, Pifferi C. 1999 Supramolecular networks via hydrogen bonding and stacking interactions for adenosine 5'-diphosphate. Synthesis and crystal structure of diaqua(2,2': 6',2''-terpyridine)copper(II) [adenosine 5'-diphosphato($^{3-}$)](2,2': 6',2''-terpyridine)cuprate(II) adenosine 5'-diphosphate($^{1-}$) hexadecahydrate and density functional geometry optimization analysis of copper(II)- and zinc(II)-pyrophosphate complexes. *J Chem Soc Dalton Trans* 699–710.
- Cotton and Wilkinson. (eds) 1988. Advanced Inorganic Chemistry, New York: John Wiley and Sons.
- De Vizcaya-Ruiz A, Rivero-Muller A, Ruiz-Ramirez L *et al.* 2000 Induction of apoptosis by a novel copper-based anticancer compound, Casiopeina II, in L1210 murine leukaemia and CH1 human ovarian carcinoma cells. *Toxicol in Vitro* **14**, 1–5.
- Gokhale N, Padhye S, Rathbone D *et al.* 2001 The crystal structure of first copper(II) complex of a pyridine-2-carboxamidrazone – a potential antitumor agent. *Inorg Chem Commun* **4**, 26–29.
- Guo Z, Sadler PJ. 1999 Metals in medicine. *Angew Chem Int Ed* **38**, 1513–1531.
- Guo Z, Sadler PJ. 2000 Medicinal inorganic chemistry. *Adv Inorg Chem* **49**, 183–306.
- Herrero LA, Terrón A. 2000 Interactions in solution of calcium(II) and copper(II) with nucleoside monophosphates: a calorimetric study. *J Biol Inorg Chem* **5**, 269–275.

- Kaska WC, Carrans C, Michalowski J, Jackson J, Levinson W. 1978 Inhibition of RNA dependent DNA-polymerase and malignant transforming ability of Rous-Sarcoma virus by thiosemicarbazone transition metal-complexes. *Bioinorg Chem* **8**, 225–236.
- Kong DY, Meng LH, Ding J, Xie YY, Huang XY. 2000 New tetraazamacrocyclic ligand with neutral pendent groups 1,4,7,10-tetrakis(2-cyanoethyl)-1,4,7, 10-tetraazacyclododecane (L) and its cobalt(II), nickel(II) and copper(II) complexes: synthesis, structural characterization and antitumor activity. *Polyhedron* **19**, 217–223.
- Leung WH, Ma JX, Yam VWW, Che CM, Poon CK. 1991 Syntheses, electrochemistry and reactivities of pyridine amide complexes of chromium (III) and manganese (III). *J Chem Soc Dalton Trans* 1071–1076.
- Lüth MS, Kapinos LE, Song B, Lippert B, Sigel H. 1999 Extent of intramolecular stacking interactions in the mixed-ligand complexes formed in aqueous solution by copper(II), 2,2'-bipyridine or 1,10-phenanthroline and 2'-deoxyguanosine 5'- monophosphate. *J Chem Soc Dalton Trans* 357–365.
- Madarász J, Bombicz P, Czugler M, Pokol G. 2000 Comparison of theophyllinato Cu(II) complexes of ethanolamine and diethanolamine: Part 2. Structure and thermal study of the dimeric complex with diethanolamine. *Polyhedron* **19**, 457–463.
- Mahadevan S, Palaniandavar M. 1998 Spectroscopic and voltammetric studies on copper complexes of 2,9-dimethyl-1,10-phenanthrolines bound to calf thymus DNA. *Inorg Chem* **37**, 693–700.
- Mazumder A, Sutton CL, Sigman DS. 1993 1,10-phenanthroline-linked *Escherichia Coli* Trp repressor as a site-specific scission reagent metal ion requirement. *Inorg Chem* **32**, 3516–3520.
- Mohindru A, Fisher JM, Rabinovitz M. 1983 Bathocuproine Sulfonate – A tissue culture -compatible indicator of copper-mediated toxicity. *Nature (London)* **303**, 64–65.
- Moubaraki B, Murray KS, Ranford JD, Vittal JJ, Wang X, Xu Y. 1999 Preparation, characterisation and structures of copper(II) complexes of an asymmetric anti-cancer drug analogue. *J Chem Soc Dalton Trans* 3573–3578.
- Ranford JD, Sadler PJ, Tocher DA. 1993 Cytotoxicity and antiviral activity of transition-metal salicylato complexes and crystal structure of bis(diisopropylsalicylato)(1,10-phenanthroline)copper(II). *J Chem Soc Dalton Trans* 3393–3399.
- Rowland JM, Thornton ML, Olmstead MM, Mascharak PK. 2001 Structure variation due to ligand flexibility: Syntheses and structures of the copper(II) complexes [Cu(APPy)] and [Cu-2(AEPy)(2)] where APPyH(2) = bis[3-(2-pyridinecarboxamido)propyl]methylamine and AEPyH(2) = bis[3-(2-pyridinecarboxamido)ethyl]methylamine. *Inorg Chem* **40**, 1069–1073.
- Ruiz-Ramírez L, De La Rosa ME, Gracia-Mora I *et al.* 1995 Casiopeinas, metal-based drugs a new class of antineoplastic and genotoxic compounds. *J Inorg Biochem* **59**, 207–207.
- Ruiz-Ramírez L, Gracia-Mora I, De La Rosa ME *et al.* 1993 Cytostatic, mutagenic, antineoplastic activities and preliminary toxicity of copper(II) new drugs: Casiopeinas I, II, III. *J Inorg Biochem* **51**, 406–406.
- Sheldrick GM. 1996 SAINT v4 Software reference manual, Siemens Analytical X-ray Systems. Madison, WI.
- Sheldrick GM. 1996 SADABS, Program for empirical absorption correction of area detector data. Germany: University of Göttingen.
- Sheldrick GM. 1996 SHELXTL, v5 reference manual, Siemens Analytical X-ray Systems. Madison, WI.
- Sigman DS. 1990 Chemical Nucleases. *Biochemistry* **29**, 9097–9105.
- Sigman DS, Bruice TW, Mazumder A, Sutton CL. 1993 Targeted Chemical Nucleases. *Acc Chem Res* **26**, 98–104.
- Skehan P, Storeng R, Scudiero D *et al.* 1990 New colorimetric cytotoxicity assay for anticancer-drug screening. *J Natl Cancer Inst* **82**, 1107–1112.
- West DX, Owens MD. 1998 Copper(II) complexes of formyl- and acetylpyrazine N(4)-(2-methylpyridinyl)-, N(4)-(2-ethylpyridinyl)- and N(4)-methyl(2-ethylpyridinyl)thiosemicarbazones. *Transition Met Chem* **23**, 87–91.
- Wilson AJ. 1992 International Table for X-ray Crystallography. Vol. C, Kluwer Academic Publishers, Dordrecht, Tables 6.1.1.4 (p.500) and 4.2.6.8 (p.219), respectively.
- Yergey JA. 1983 A general-approach to calculating isotopic distributions for mass-spectrometry. *Int J Mass Spectrom Ion Phys* **52**, 337–349.
- Zhang JY, Liu Q, Xu Y, Zhang Y, You XZ, Guo ZJ. 2001 N-(8-quinolyl)pyridine-2-carboxamide. *Acta Cryst* **C57**, 109–110.